Cellular Signalling 53 (2019) 294–303

Contents lists available at ScienceDirect

Cellular Signalling

journal homepage: www.elsevier.com/locate/cellsig

Thiamethoxam inhibits blastocyst expansion and hatching via reactive-oxygen species–induced G2 checkpoint activation in pigs

Zheng-Wen Nie[1], Ying-Jie Niu[1], Wenjun Zhou, Yong-Han Kim, Kyung-Tae Shin, Xiang-Shun Cui*

Department of Animal Sciences, Chungbuk National University, Chungbuk, Cheongju 361-763, Republic of Korea

ARTICLE INFO

Keywords:
Thiamethoxam
Porcine blastocyst
ROS
DNA damage
Cell cycle

ABSTRACT

Thiamethoxam (TMX) is a neonicotinoid insecticide. It has specific high toxicity to insects. Residues of TMX have been detected in various crops. Early embryo quality is vital for fertility. Excessive production of reactive oxygen species (ROS) can override embryonic antioxidant defenses, producing oxidative stress that triggers apoptosis, necrosis, and/or permanent DNA damage responses in the early embryo. Comparative studies have indicated that TMX hepatotoxicity is significant in mammals in acute tests, but little is known about accumulated chronic toxicity in early embryonic development. Porcine embryos were obtained here by the parthenogenetic activation of meiosis II oocytes and cultured in the PZM-5 medium with or without TMX. These embryos were evaluated by various methods. The expansion and hatching of blastocysts treated with TMX decreased by 21.73% and 16.71%, respectively, as compared with controls. In an analysis of 5-bromo-2-deoxyuridine (BrdU) incorporation, the rate of cell proliferation was 44.33% lower as compared with expanded blastocysts of the control group. ROS and γH2AX levels were higher in the TMX group than in the control group. Real-time reverse-transcription polymerase chain reaction showed that Sod1 expression increased and the expression of Mnsod, Gpx1, Igta5, and Cox2 decreased. A CDK1 kinase assay revealed that maturation-promoting factor (MPF) activity diminished by 31.41% in expanding blastocysts. In conclusion, these results suggest that TMX inhibits blastocyst expansion and hatching by ROS-induced DNA damage checkpoint activation, which inhibits the activation of MPF and cell cycle progression in porcine blastocysts.

1. Introduction

Neonicotinoids are applied at various crop stages and during post-harvest storage and play important roles in food security and quality preservation. They are the fastest growing class of insecticides [1] and act selectively on the central nervous system of insects, with minimal effects on beneficial insects and with low toxicity toward mammals, including a lack of teratogenic or mutagenic effects [2]. Among these insecticides, imidacloprid (IMI), thiamethoxam (TMX), thiacloprid (THI), nitenpyram (NIT), acetamiprid (ACE), and clothianidin (CLO) are most widely used [3]. However, they have an inherent degree of embryotoxicity, and TMX has a significantly greater effect on early embryonic development at a low concentration as compared to THI, ACE, and CLO in mice and rabbits [4]. Nevertheless, the mechanism by which the toxicity of TMX decreases the developmental potential of mammals at the molecular level is still unknown. In addition, residues of TMX have been detected in various crops, such as rice hulls, bran, and polished rice grains, and the highest concentrations have been observed in hulls and in rice bran [5]. Therefore, it is necessary to further investigate the mechanisms underlying the toxicity of TMX.

The pig, a traditional livestock species, is a major source of meat. Porcine reproductive performance is frequently investigated to acquire large farrows. Early embryo quality is vital for porcine fertility. Factors that influence embryo quality—such as cleavage interruption, cavity failure, hatching failure, and embryonic death—can induce pregnancy failure. Therefore, porcine preimplantation embryos were employed to evaluate TMX toxicity in this study.

A large amount of oxygen, which is proportional to the concentrations of reactive oxygen species (ROS), has detrimental effects on early embryos, and the effects on precompaction embryos are irreversible, with the stress culminating in a significant loss of viability post-implantation [6–9]. Excessive production of ROS can override antioxidant defenses in embryos, thus yielding oxidative stress that triggers apoptosis, necrosis, and/or permanent cell cycle arrest in the developing early embryo [10–13]. Oxidative stress can affect the DNA damage response either by the direct production of several DNA lesions,

* Corresponding author.
E-mail address: xscui@cbnu.ac.kr (X.-S. Cui).
[1] These authors contributed equally to this study.

https://doi.org/10.1016/j.cellsig.2018.08.014
Received 16 July 2018; Received in revised form 22 August 2018; Accepted 22 August 2018
Available online 24 August 2018
0898-6568/

necessitating different DNA repair pathways, or by modifying key repair proteins, thereby decreasing DNA binding; additionally, both ROS/RNS-mediated DNA damage and the redox-mediated inhibition of DNA damage response proteins can cause structural alterations in DNA; these alterations if unrepaired lead to the formation of mutations and/or apoptosis [14]. In the zebrafish liver, TMX increases ROS levels, whereas catalase (CAT), superoxide dismutase (SOD), and glutathione *S*-transferase (GST) are activated at an early exposure time point. The antioxidant defense system functions but is not sufficient. In addition, TMX and the resulting ROS at a high concentration of the drugs over long periods result in severe DNA damage [15]. In mice, TMX blocks early embryonic development before the blastocyst stage, reduces the total cell number, and increases the number of dead cells in blastocysts [4].

In the present study, it was hypothesized that TMX impedes porcine preimplantation embryonic development via an ROS-dependent DNA damage checkpoint response.

2. Materials and methods

2.1. Oocyte collection, in vitro maturation, and embryo culture

Ovaries from prepubertal gilts were obtained from a local slaughterhouse, maintained in saline at 37 °C, and transported to the laboratory. Cumulus oocyte complexes were isolated from follicles and washed three times in Tyrode's lactate-4-(2-hydroxyethyl)-1-piperazineethanesulfonic acid. The cumulus oocyte complexes were cultured in tissue culture medium 199 (TCM 199) supplemented with 10% of porcine follicular fluid, 0.1 g/l sodium pyruvate, 0.6 mM L-cysteine, 10 ng/ml epidermal growth factor, 10 IU/ml luteinizing hormone, and 10 IU/ml follicle-stimulating hormone at 38.5 °C for 44 h in a humidified atmosphere of 5% CO_2 and 95% air. After maturation, cumulus cells surrounding oocytes were removed by treatment with 0.1% hyaluronidase for ~1 min and repeated pipetting. For parthenogenetic activation, oocytes with first polar bodies were selected and activated by two direct current (DC) pulses of 1.1 kV/cm for 60 μs and then incubated in a porcine zygote medium (PZM-5) containing 7.5 μg/ml cytochalasin B for 3 h. Finally, the embryos were cultured in the PZM-5 medium for 7 days at 38.5 °C in a humidified atmosphere of 5% CO_2 and 95% air. On the fifth day, fetal bovine serum was added to the medium to a total concentration of 10%. To observe the effect of TMX (37,924; Sigma, St. Louis, MO, USA) on porcine early embryonic development, TMX was added to the medium. For a BrdU incorporation assay, embryos were exposed to 100 μM BrdU in the medium for 6 h before cultivation was completed.

2.2. Immunofluorescent staining and confocal microscopy

Embryos were fixed in 3.7% paraformaldehyde for 1 h at room temperature, washed three times with phosphate-buffered saline/polyvinyl alcohol (PBS/PVA), permeabilized with PBS/PVA containing 1.0% Triton X-100 at 37 °C for 1 h, and washed three times with PBS/PVA. For the TUNEL assay, embryos were incubated with terminal deoxynucleotidyl transferase (In Situ Cell Death Detection Kit; Roche, Basel, Switzerland) in the dark for 1 h at 38.5 °C. For the BrdU incorporation assay, permeabilized embryos were treated with PBS containing 2 N HCl for 40 min and washed three times with PBS/PVA. Then, all the embryos were blocked in PVA-PBS containing 1.0% of bovine serum albumin at 37 °C for 1 h. Subsequently, the embryos were incubated overnight at 4 °C with an anti-γH2AX antibody (pS139, 1:100; Cell Signaling Technology, Danvers, MA, USA), anti-ATM antibody (pS1981, 1:100; Cell Signaling Technology), anti-CDC25C antibody (sc-5620, 1:100; Santa Cruz Biotechnology, Dallas, TX, USA), anti-TOM20 antibody (sc-17764, 1:200; Santa Cruz Biotechnology), anti-P53 antibody (sc-6243, 1:100; Santa Cruz Biotechnology), anti-P21 antibody (P1484, 1:100; Sigma-Aldrich), or an anti-BrdU antibody. After three washes in PBS/PVA, the embryos were incubated at 37 °C for 1 h with a secondary IgG antibody, stained with Hoechst 33342 (bisBenzimide H33342 trihydrochloride, 1:2000; Sigma Life Science) for 15 min, washed three times in PBS/PVA, mounted onto slides, and examined under a confocal microscope (Zeiss LSM 710 META; Jena, Germany). Images were processed in the Zen software (version 8.0, Zeiss).

2.3. Real-time reverse-transcription polymerase chain reaction

mRNA was extracted from 30 blastocysts per group with a Dynabeads mRNA Direct Kit (DynalAsa, Oslo, Norway). The cDNAs were obtained by reverse transcription using the Express 1st Strand cDNA Synthesis System Kit (Thermo Fisher Scientific, Waltham, MA, USA) and amplified by means of WizPure qPCR Master with the Super Green Kit (Wizbio Solutions, Seongnam, South Korea). The amplification cycling conditions were as follows: 95 °C for 10 min; followed by 40 cycles of 95 °C for 15 s, 55 °C or 60 °C for 25 s, and 72 °C for 10 s; and final extension at 72 °C for 5 min. The relative gene expression levels were normalized to internal porcine *Gapdh* mRNA levels by the $2^{-\Delta\Delta CT}$ method. The sequences of primers for Sod1 were 5′-GAGACCTGGGCA ATGTGACT-3′ (forward) and 5′-CCAAACGACTTCCAGCATTT-3′ (reverse). The other primers used for RT-PCR were from previous studies [16,17].

2.4. ROS and mitochondrial peroxide staining

The ROS contents of the treated and untreated embryos were measured at the blastocyst stage. ROS content was quantified by the dichlorodihydrofluorescein diacetate (DCHFDA, Molecular Probes, Invitrogen, Carlsbad, CA, USA) method, as described elsewhere (31). For mitochondrial peroxide staining, embryos were incubated in MitoSOX Red Mitochondrial Superoxide Indicator diluted with the PZM-5 medium (M36008, 1:250; Thermo Fisher Scientific) for 30 min and then washed three times with PBS/PVA. Live imaging and quantitation were conducted using a fluorescence microscope (Nikon, Tokyo, Japan) and Photoshop (CS2; Adobe, San Jose, CA, USA).

2.5. Western blot analysis

Each sample contained 150 porcine blastocysts in 15 μl SDS sample buffer and was heated at 95 °C for 10 min. Proteins were separated by SDS-PAGE according to molecular weight and transferred to polyvinylidene fluoride membrane. The membrane was cut into different regions according to the positions of detected proteins. These fragments of membrane were blocked in Tris-buffered saline (TBS) containing 0.1% Tween 20 and 5% skim milk for 1 h, incubated at 4 °C overnight with rabbit anti-CHK1 (1:1000; ab47318; Abcam), mouse anti-CDK2 (1:1000; MA5-17052; Thermo Scientific) or mouse anti-β-actin antibodies (1:1000; 3700; Cell Signaling Technology), washed three times with (TBS) containing 0.1% Tween 20 and then incubated with horseradish peroxidase-conjugated goat anti-rabbit or anti-mouse IgG (1:2000; Santa Cruz Biotechnology) at room temperature for 1 h. The contents of proteins were detected with Pierce ECL Western blotting substrate (Thermo Fisher Scientific). To quantify these proteins, band intensity values were determined using Image J software.

2.6. An in vitro p34cdc2 kinase (CDK2) assay

The embryos were exposed to 20 ng/ml colcemid 12 h before the collection of samples. Thirty embryos, as a sample, were lysed with 5 μl of sample buffer (50 mM Tris-HCl [pH 7.5], 0.5 M NaCl, 5 mM EDTA, 2 mM EGTA, 0.01% Brij-35 (v/v), 1 mM PMSF, 0.05 mg/ml leupeptin, 50 mM 2-mercaptoethanol, 25 mM β-glycerophosphate, and 1 mM sodium orthovanadate) and stored at −80 °C. Embryo extracts were quantified by an ELISA via the MESACUP cdc2 Kinase Assay Kit (MBL

International, Nagoya, Japan), and the optical density of each well was read at 492 nm on a microplate reader.

2.7. Statistical analysis

All data were presented as the mean ± standard error of mean (SEM). The differences between the treatment groups were assessed by the least significant difference test in the Statistical Package for Social Sciences (SPSS) software. Fluorescent intensity of DNA and p53 signals was calculated with Image J in Fig. 5c. The difference between 2 groups was analyzed with paired sample *t*-test. The significant difference ($p < .05$) and the great significant difference ($p < .01$) were respectively marked with "*" and "**". As for comparison among > 2 groups, one-way ANOVA was used to analyze the difference and the difference was marked with lowercases. There was significant difference ($p < .05$) if no same lowercases between groups. Each experiment was conducted at least in triplicate. The relative value of each repeat in the control group or score 4–6 group was set to 1.

3. Results

3.1. TMX inhibited blastocyst expansion and hatching

To determine the toxicity of TMX during early embryonic development, a concentration gradient of TMX was set up. Early embryos were exposed to various concentrations of TMX during preimplantation development to determine the proper concentration of TMX. To get a high blastocysts rate and further investigate the development of blastocysts such as expanding and hatching, these embryos were cultured for 7 d [18,19]. When embryos were cultured for 7 d, a high concentration of TMX did not appear to have an effect on the number of blastocysts (Fig. 1a). These blastocysts were next subdivided into 6 classes based on a score from 1 to 6 according to the criteria established by Gardner [20]. When blastocysts were stained with Hoechst 33342, the majority of them with a score of 1 had few nuclei, and the nuclei were irregular. These results indicated that blastocysts with a score of 1 were dead on the seventh day. Therefore, these dead blastocysts were removed from the total blastocysts, and the blastocyst rate was calculated. TMX at a concentration of 1.6 mM decreased the blastocyst rate significantly (47.68 ± 1.12% vs. 29.25 ± 1.23%, $p < .05$, Fig. 1b). In addition, blastocysts in the TMX group were smaller than those in the control group, as evidenced by the significant reduction in expanded blastocysts (score 4, 21.73 ± 6.02% vs. 0%, $p < .05$) in the TMX group. There were no full-size (score 4–6, 40.36 ± 2.28% vs. 0%, $p < .01$) and hatching or hatched blastocysts (score 5–6), but there were much more unexpanded and expanding blastocysts in the TMX group than in the control group (score 2–3, 40.17 ± 2.75% vs. 55.67 ± 5.97%, $p < .05$, Fig. 1a, c, d). These results suggested that TMX treatment could effectively inhibit blastocyst expansion and subsequent hatching.

3.2. TMX inhibited the proliferation of blastocysts

Blastocysts of different sizes contain different numbers of cells. Therefore, cell proliferation was evaluated by a 5-bromo-2′-deoxyuridine (BrdU) incorporation assay. As blastocysts grew, the number of cells detected by Hoechst 33342 staining increased. Compared to blastocysts with score 3, the cell counts for blastocysts with a score of 4–6 were significantly higher in the control group (99.67 ± 5.36 vs. 51.00 ± 4.04, $p < .05$), but there was no difference between the control and TMX group at the same score (score 2: 28.00 ± 1.73 vs. 24.33 ± 4.81; score 3: 51.00 ± 4.04 vs. 55.33 ± 4.81, Fig. 2a, b). Nevertheless, the number of nuclei according to BrdU fluorescence was significantly lower in the TMX group than in the control group for score

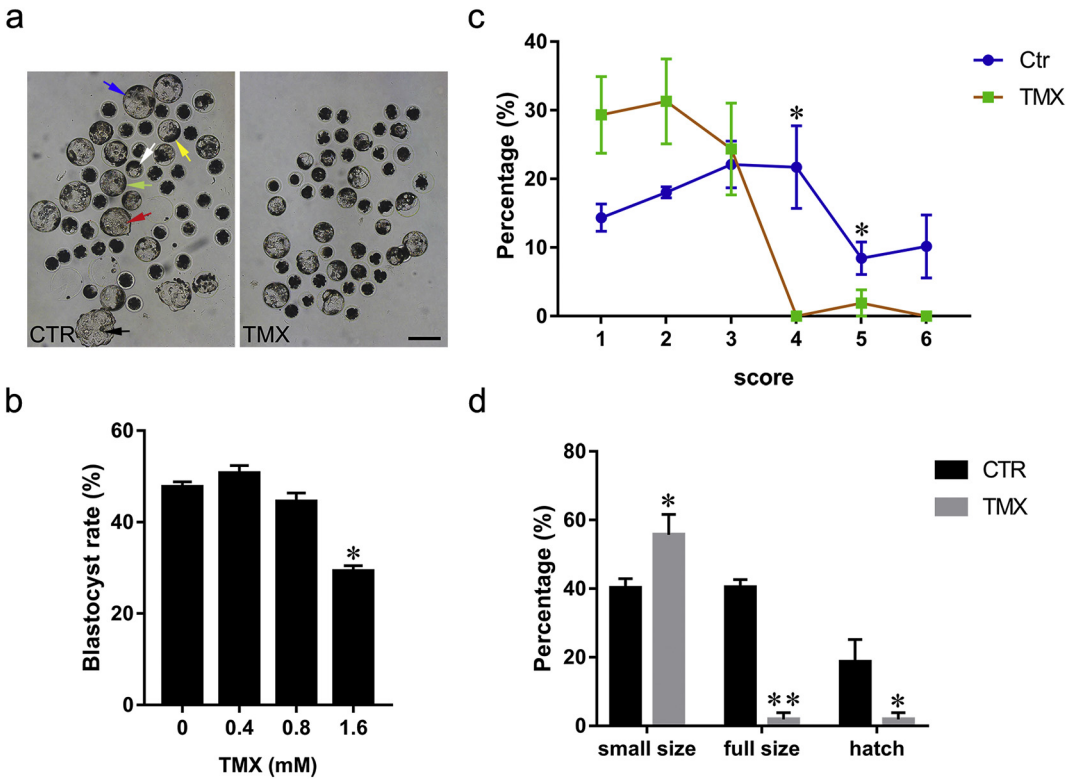

Fig. 1. Effect of TMX toxicity on porcine blastocyst formation. (**a**) Blastocyst morphology at 7 d. The white arrow: score 1, the yellow arrow: score 2, the green arrow: score 3, the blue arrow: score 4, the red arrow: score 5, and the black arrow: score 6. Scale bar = 200 μm. (**b**) Effects of TMX at various concentrations on blastocyst rates. (**c**) Percentages of blastocysts exposed to TMX for each score. (**d**) The influence of TMX on the size and hatching of blastocysts. Small size: score 2–3; full size: score 4–6; hatch: score 5–6. (For interpretation of the references to colour in this figure legend, the reader is referred to the web version of this article.)

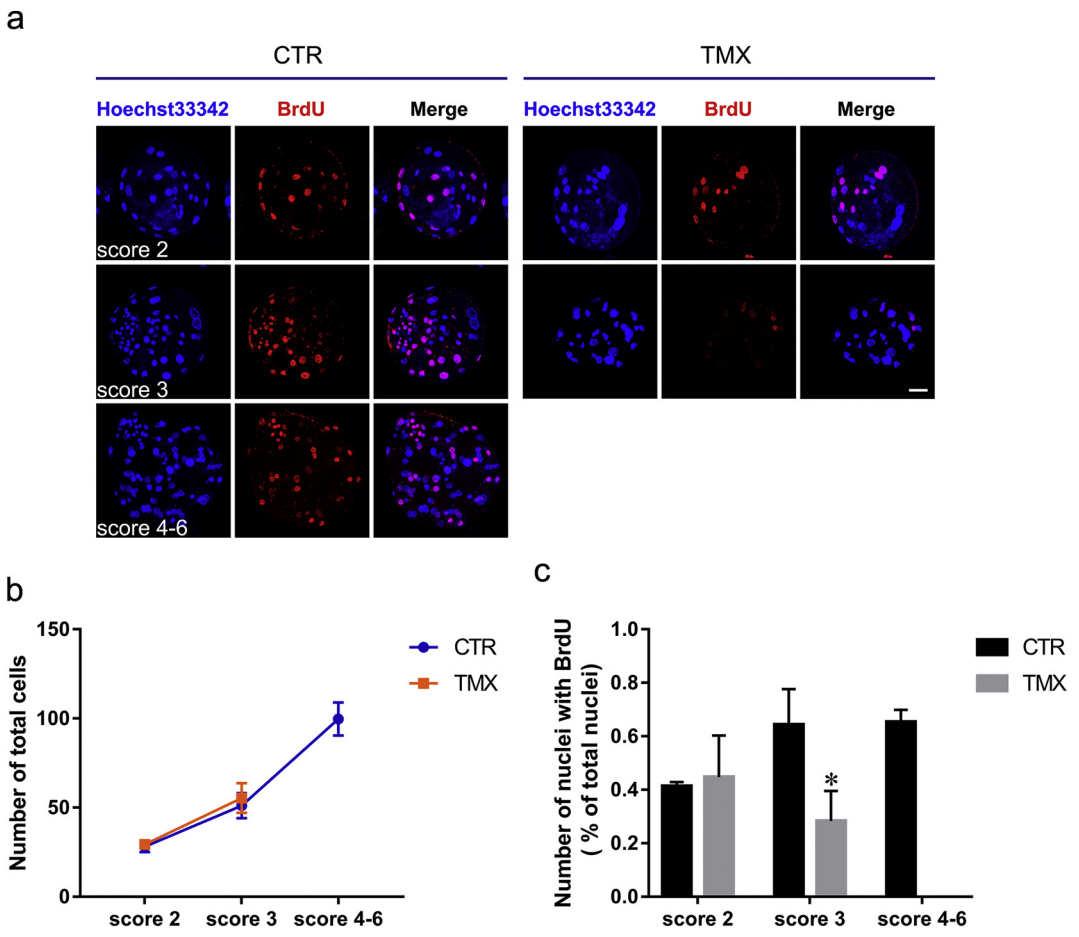

Fig. 2. Cell proliferation in blastocysts exposed to TMX. (**a**) Immunofluorescence staining of BrdU in blastocysts. Scale bar = 35 μm. (**b**) Total cell numbers for individual blastocysts. (**c**) The numbers of cells with BrdU staining in a blastocyst.

3 (64.33 ± 7.69% vs. 28.33 ± 6.48%, $p < .05$, Fig. 2a, c). These results indicated that the stage corresponding to score 3 is the start of extensive proliferation, and TMX mainly inhibits cell proliferation at this stage.

3.3. Increased ROS production resulted from TMX

The ROS content of blastocysts was determined. A greater average relative intensity of DCDHF per blastocyst was found in the TMX group than in the control group (64.33 ± 7.69 vs. 28.33 ± 6.48, $p < .05$, Fig. 3a, b). This finding suggested that TMX induced the production of ROS. Then, mitochondria in blastocysts were tracked with MitoSOX and TOM20, which are markers of superoxide-rich and all mitochondria, respectively. Compared to the control group, blastocysts in the TMX group had a higher ratio of the MitoSOX to TOM20 signal intensity (0.61 ± 0.04 vs. 1.09 ± 0.12, $p < .05$, Fig. 3c, d). In addition, although mitochondria tracked by TOM20 were in the cytoplasm in both the control and TMX groups, MitoSOX signals in the blastocysts exposed to TMX had nuclear localization (Fig. 3c). These results indicated that the large amount of superoxide induced by TMX may bind to nucleic acids and have an effect on DNA in the nucleus. The expression of genes related to ROS, such as *Sod1*, *Mnsod,* and *Gpx1*, was analyzed by RT-PCR (Fig. 3e). The mRNA levels of all of these genes increased significantly from score 2–3 to score 4–6 in the control group. *Sod1* mRNA levels were higher in the TMX group than at a score of 2–3 in the control group (0.55 ± 0.09 vs. 1.47 ± 0.02, $p < .05$). By contrast, mRNA levels of *Mnsod* and *Gpx1* did not differ between groups "control" and "TMX" at score 2–3, although there was a significant difference between the control group at score 4–6 and the TMX group at score 2–3. These results indicated that high expression levels of *Sod1*, *Mnsod,* and *Gpx1* are necessary for blastocyst growth and hatching, and in response to increased ROS amounts induced by TMX, the rapid increase in *sod1* expression cannot reverse the situation.

3.4. The DNA damage checkpoint induced by TMX influenced blastocysts

According to the localization of superoxide in cell nuclei of blastocysts, we speculated that DNA might be damaged in the TMX group. Therefore, DNA damage was evaluated by γH2AX staining. The relative number of nuclei with γH2AX signals in score 2–3 of TMX group (33.52 ± 2.82) was greater than the number of score 2–3 (8.16 ± 1.26, $p < .01$) or score 4–6 (4.84 ± 1.51, $p < .05$) of the control group (Fig. 4a, b). This result supports our speculation. On the other hand, there were no obvious differences in terminal deoxynucleotidyl transferase (TdT) dUTP nick-end labeling (TUNEL) signals between the groups, suggesting that the DNA damage was not sufficiently severe to trigger apoptosis (Fig. 4a). Next, to clarify whether the DNA damage checkpoint is functional, the related pathways were evaluated. Immunofluorescent staining of phosphorylated ataxia-telangiectasia mutated (ATM) showed that the amounts of phosphorylated ATM in nuclei were significantly greater in the TMX group compared to those in the control group for a score of 2–3 or 4–6 (Fig. 4c, d). Subsequent western blot blotting showed revealed increased upregulation of checkpoint kinase 1 (CHK1) at in the TMX group (Fig. 4e, f). CDC25C levels were also significantly increased compared to those for score 2–3 in the control (Fig. 4g, h). The active ATM caused by DNA damage positively regulated CHK1 and inhibited CDC25C. In addition, the p53–p21 pathway also played a role in this checkpoint, as evidenced by

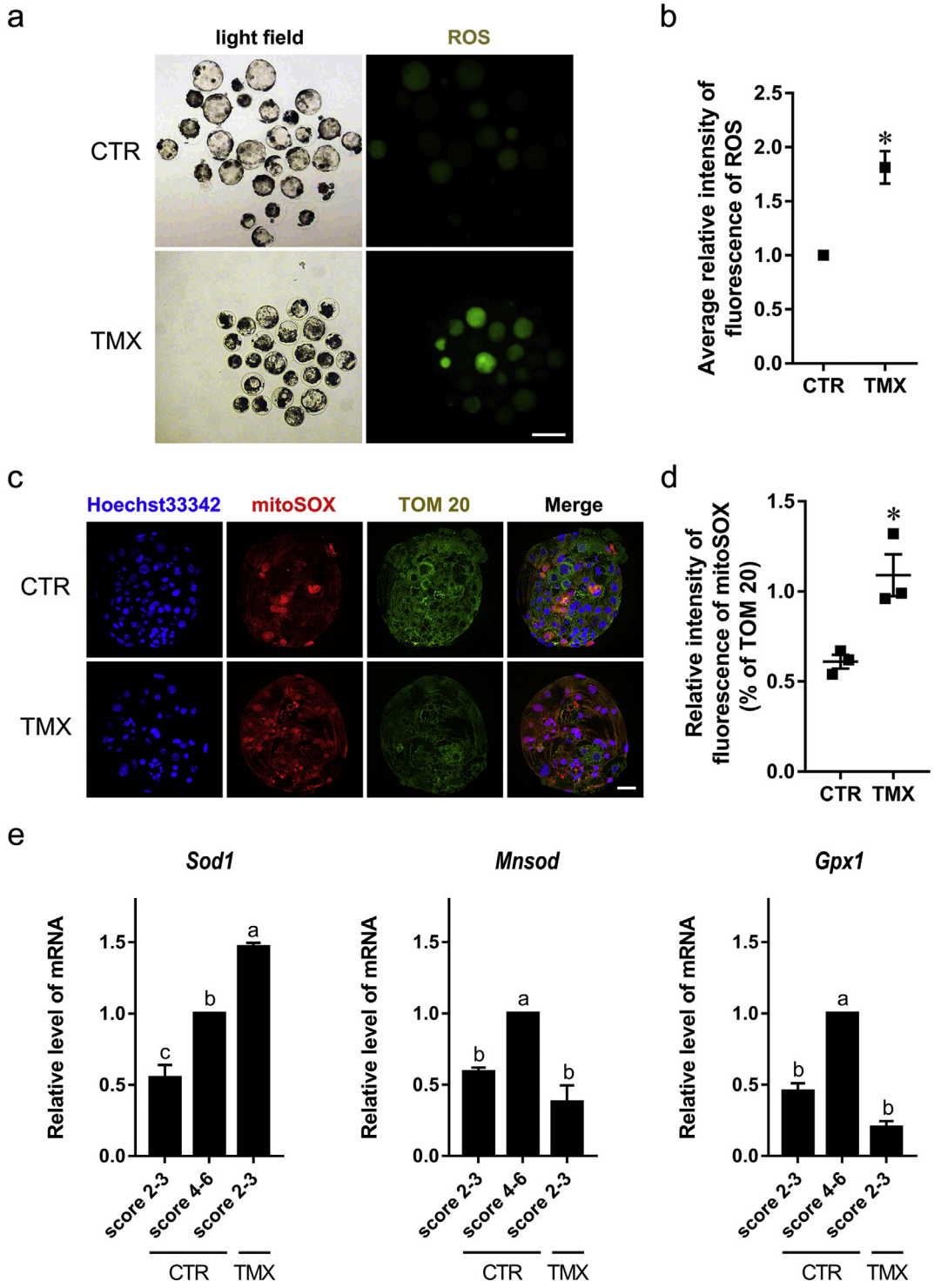

Fig. 3. Oxidative stress in blastocysts exposed to TMX. (**a**) DCHFDA staining for ROS in blastocysts. Scale bar = 200 μm. (**b**) The relative average level of ROS in a blastocyst. (**c**) Peroxide tracking with MitoSOX and immunofluorescence staining of mitochondrial TOM20. Scale bar = 35 μm. (**d**) The relative average level of peroxides in a blastocyst. (**e**) The relative mRNA levels of *Sod1*, *Mnsod*, and *Gpx1*. The value of control group or score 4–6 group was set to 1.

the increased localization of p53 in the cytoplasm (Fig. 5a–c) and p21 in nuclei (Fig. 5d, e) in nuclei in the TMX group compared to the score 4–6 control group. These findings indicated that the DNA damage checkpoint is important for the blastocyst response to TMX toxicity.

3.5. DNA damage was caused by increased ROS amounts

According to some studies [21,22], it is possible that ROS production induced by TMX triggers DNA damage. To verify this hypothesis, blastocysts in the TMX group were exposed to 10 μM KU55933 (an ATM inhibitor) [23] or 1 μM β-mercaptoethanol (an ROS inhibitor) [22]. As presented in Fig. 6a–c, β-mercaptoethanol attenuated the TMX-induced increases in ROS and phosphorylated ATM amounts (1.74 ± 0.16 vs. 1.02 ± 0.15, $p < .05$; 1.71 ± 0.08 vs. 1.28 ± 0.32, $p < .05$). By contrast, KU55933 could not decrease the large amount of ROS caused by TMX but reduced the amount of

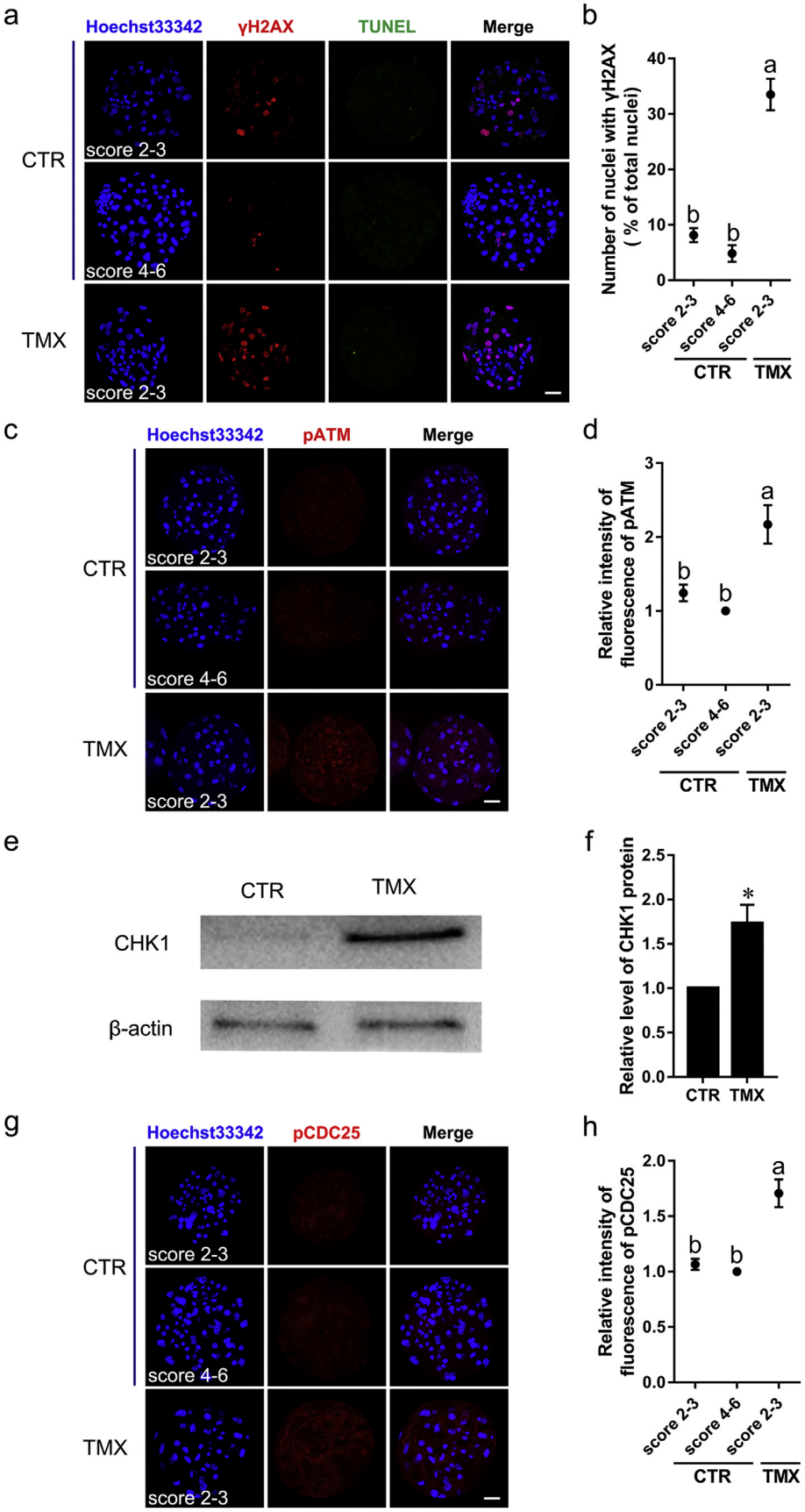

Fig. 4. The ATM-CHK1-CDC25C pathway of DNA damage checkpoint in blastocysts exposed to TMX. (**a**) γH2AX and TUNEL staining. (**b**) Numbers of cells with γH2AX staining in a blastocyst. (**c**) Immunofluorescent staining of phosphorylated ATM. (**d**) The relative average amount of phosphorylated ATM in a blastocyst. (**e**) Immunofluorescence staining of CHK1. (**f**) The relative level of CHK1 protein. (**g**) Immunofluorescent staining of phosphorylated CDC25. (**h**) The relative intensity of phosphorylated CDC25. The value of control group or score 4–6 group was set to 1. Scale bar = 35 μm.

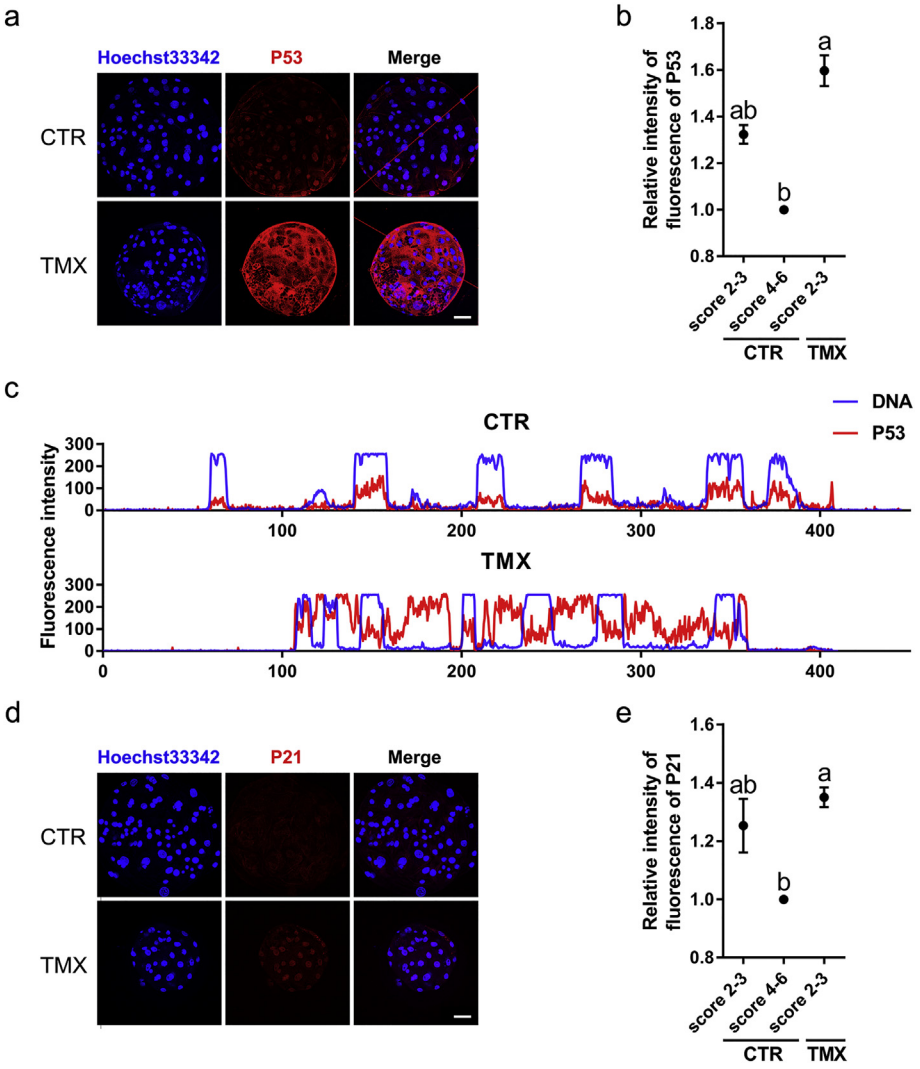

Fig. 5. The p53-p21 pathway of DNA damage checkpoint in blastocysts exposed to TMX. (**a**) Immunofluorescence staining of p53. (**b**) The relative average amount of p53 in a blastocyst. (**c**) Fluorescent intensity of DNA and p53 signals at the red line in Fig. 5a. (**d**) Immunofluorescence staining of p21. (**e**) The relative average level of p21 in a blastocyst. The value of score 4–6 group was set to 1. Scale bar = 35 μm. (For interpretation of the references to colour in this figure legend, the reader is referred to the web version of this article.)

phosphorylated ATM (1.74 ± 0.16 vs. 1.95 ± 0.20, $p > .05$; 1.71 ± 0.08 vs. 1.20 ± 0.17, $p < .05$).

3.6. The cell cycle was blocked by G1 and G2 phase arrest

CDK2-cyclin E complex regulates G1/S transition and CDK2 can negatively respond to DNA damage checkpoint [24]. Therefore, the western blotting was performed and the result showed the significantly decreased level of CDK2 in TMX group compared to the control (Fig. 7a, b). Moreover, Active maturation-promoting factor (MPF), consisting of CDK1 and cyclin B, is vital for the entry into mitosis metaphase from G2 phase [25], and CDK1 is a target of the DNA damage checkpoint response [26]. Therefore, the activity of CDK1 was likely to be repressed by a functional DNA damage checkpoint. The significantly lower activity of CDK1 in the TMX group as compared with score 2–3 or 4–6 in the control group was consistent with the expectation (Fig. 7c). In addition, genes related to blastocyst expansion and hatching, e.g., *Fn1*, *Igta5*, and *Cox2*, were also evaluated. *Fn1* was not significantly affected by TMX, but the expression levels of *Igta5* and *Cox2* were significantly lower in the TMX group than in score 4–6 controls (Fig. 7d).

4. Discussion

Neonicotinoids, such as imidacloprid, TMX, and nitenpyram, act as agonists against nicotinic acetylcholine receptors (nAChRs), but they possess immunotoxicity, hepatotoxicity, and nephrotoxicity and have antireproductive cytotoxic effects on animals via increased ROS or RNS formation in vivo [27–29]. Xu et al. have evaluated the mechanism underlying neonicotinoid adverse effects [30] and found that neonicotinoids can attack mitochondria, and then the impaired mitochondria produce increased amounts of ROS. Subsequently, the increased oxidative stress induced by ROS results in changes of antioxidant genes expression (such as Gpx and Sod), protein oxidation, lipid oxidation, DNA oxidation, function of androstane receptor and pregnane X receptor and activation of ERK and p38. Finally, hepatocellular proliferation, a carcinogenic potential, apoptosis, and DNA damage increase. TMX induces oxidative stress and an antioxidant response in the zebrafish liver [15]. In the present study, TMX induced high levels of ROS as determined by DCHFDA levels, consistent with these previous studies. In addition, hyperoxides, as evaluated by means of MitoSOX, in the TMX group showed strong colocalization with DNA. 8-Hydroxydeoxyguanosine (8-OHdG), an oxidized form of guanine, produced by ROS can be incorporated by DNA polymerases into a DNA strand

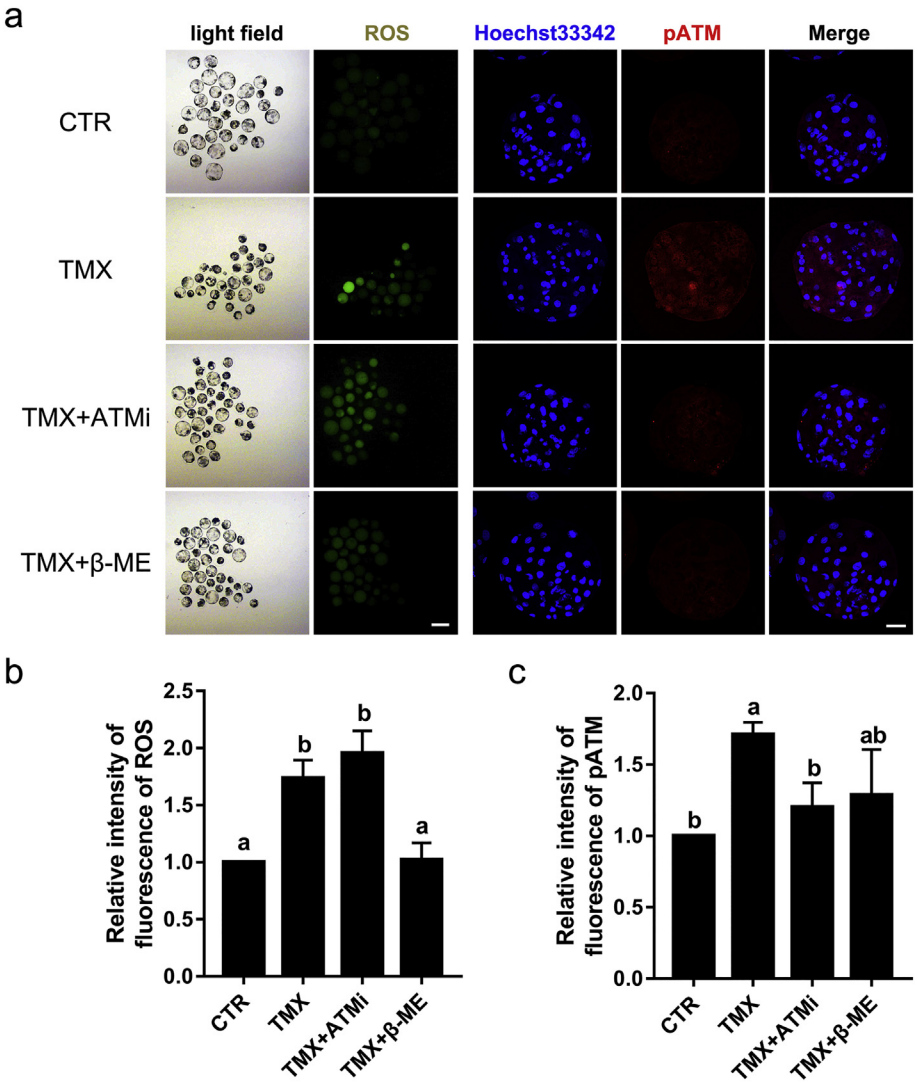

Fig. 6. The ROS-dependent DNA damage checkpoint in blastocysts exposed to TMX. (**a**) DCHFDA staining and immunofluorescent staining of phosphorylated ATM after KU55933 or β-mercaptoethanol treatment. Left scale bar = 200 μm. Right scale bar = 35 μm. (**b**) Relative levels of ROS after KU55933 or β-mercaptoethanol treatment. (**c**) A relative amount of phosphorylated ATM after KU55933 or β-mercaptoethanol treatment. The value of control group was set to 1.

from the deoxynucleotide pool [31]. Taken together with the above studies, this finding indicates that TMX can induce DNA oxidation. Consistent with the increased hyperoxide levels, *Mnsod* and *Gpx1* were expressed more weakly, but *Sod1* manifested higher expression in the TMX group than in the control group. The activity of SOD in the zebrafish liver increases on day 7 or 14 but decreases and is subsequently inhibited after exposure to TMX [15]. Therefore, the high level of *Sod1* expression may be the result of oxidative stress, and SOD1 may be the primary enzyme defending against oxidative damage induced by TMX.

In one way, ROS can cause DNA damage [32]. In particular, ROS, such as H_2O_2, can result in the oxidation of bases, DNA single-strand breaks and double-strand breaks [33,34]. In the other way, DNA damage can upregulate ROS. For example, ATM deficiency, which results in severe DNA damage, significantly reduces total antioxidant capacity [35], and cells lacking ATM are more sensitive to oxidative stress than normal cells are [36]. An ATM deficiency can lead to increased oxidative stress [37,38]. Therefore, we evaluated the causal relation by means of the ATM inhibitor KU55933 and ROS inhibitor β-mercaptoethanol. The observation that TMX resulted in ROS-induced DNA damage is in line with the former way, but inconsistent with the latter way.

The DNA damage checkpoint is involved in many cellular processes via a variety of mechanisms during the G1 phase, S phase, and G2 phase of the cell cycle [39]. The major pathways include ATM (or ATR)–CHK1 (or CHK2) and p53. The final target proteins include the Cyclin E (or A)–CDK2 complex of the G1 and S phase and the Cyclin B–CDK1 complex of the G2 phase. In the G2 phase of LCL-N cells, the p53-$p21^{waf1}$ pathway induced by DNA damage is not under the control of ATM [40]. According to another study, when telomere damage (a type of DNA damage) occurs, active ATM inhibits CDC25C by the phosphorylation of p53; as a result, the activity of the Cyclin B–CDK1 complex decreases, but the p53-$p21^{waf1}$ pathway can also inhibit Cyclin B–CDK1 directly under the control of ATM [41]. In addition to CDK1, p21 induced by p53 during DNA damage inhibits CDK2 [42]. In agreement with these previous findings, when DNA damage was observed (as determined by γH2AX), phosphorylated ATM, p53, and p21 were upregulated here, and CDC25C was downregulated. As a result, CDK1 and CDK2 were inactive or downregulated.

In addition, cytoplasmic p53 can reduce ROS levels [43]. P53 accumulates in the cytoplasm in response to DNA damage and can trigger apoptosis and inhibit autophagy [44]. Indeed, the p53 amount was reduced in nuclear fractions and aggregated in the cytoplasm of blastocyst cells in the TMX group. Nonetheless, cytoplasmic p53 in that group could not induce apoptosis. It is possible that the cytoplasmic p53

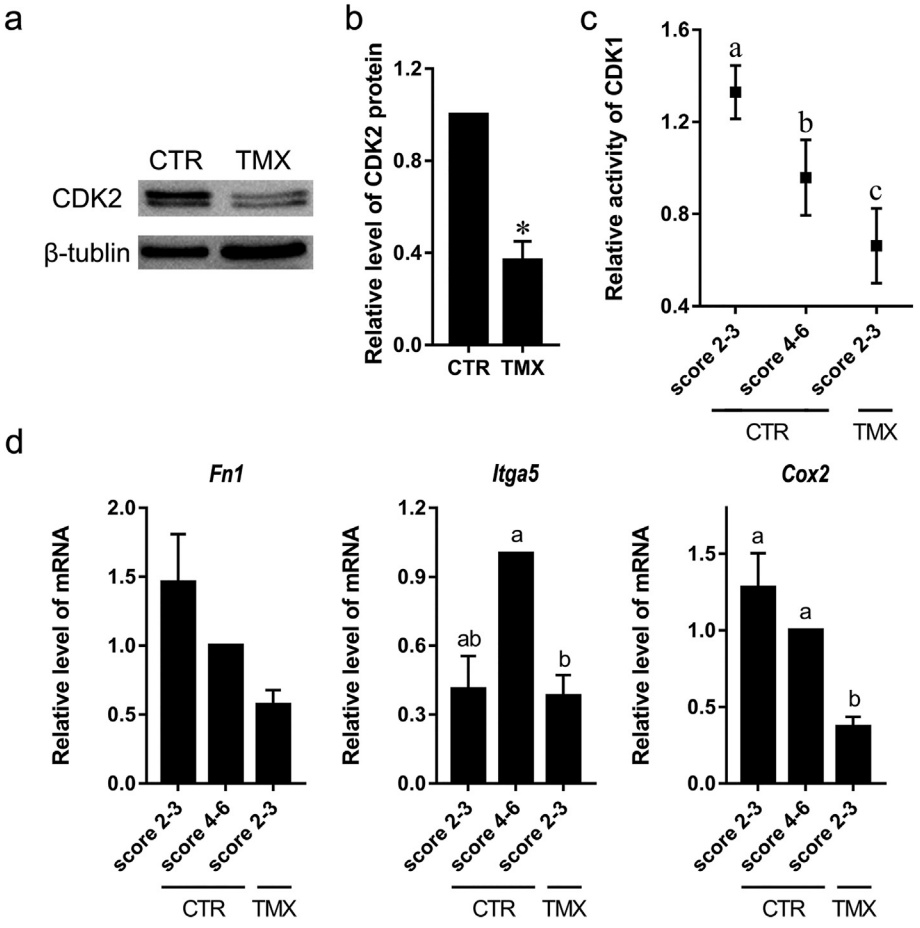

Fig. 7. Blastocysts arrested in G1 and G2 phases during exposure to TMX. (**a**) Western blotting for CDK2 and β-tubulin. (**b**) Relative levels of CDK2. (**c**) Relative activity of CDK1. (**d**) The transcript levels of *Fn1*, *Igta5*, and *Cox2*. The value of control group or score 4–6 group was set to 1.

amount increases only in response to ROS produced by mitochondria. With respect to p21, research indicates that DNA damage leads to the nuclear accumulation of p21 in HCT116 and leukemic cells [45,46]; this finding is consistent with our results. In particular, DNA damage responses are stage-specific during mouse preimplantation development; the p21-mediated cell cycle arrest starts at the midblastula transition stage [47]. Our results suggest that TMX indeed induces DNA damage checkpoint activity in blastocysts via the p53–p21 pathway.

Complexes Cyclin E–CDK2 and Cyclin B–CDK1, as regulators of the G1 phase and G2 phase, perform important functions in early embryonic development. In addition, blastocysts with score 3 are expanding, and grow rapidly through many cell cycles. Therefore, the bulk of ROS production and DNA damage occurs at this stage during blastulation. Our results show that this arrest is more frequent in blastocysts having a score of 3. As a result, blastocysts could not hatch from the zona pellucida. Decreased expression levels of genes related to hatching proved that blastocysts indeed lose their ability to hatch.

5. Conclusions

These results suggest that TMX induces oxidative stress and disrupts mitochondrial function. These changes result in an imbalance in the oxidation-reduction reaction and increased ROS amounts, which induce DNA oxidation and subsequent DNA damage. Substantial DNA damage accumulates due to rapid cell proliferation in blastocysts with a score of 3. The ROS-dependent DNA damage response arrests the cell cycle in expanding blastocysts via the ATM–CHK1–CDC25C and ATM–p53–p21 pathways (Fig. 8).

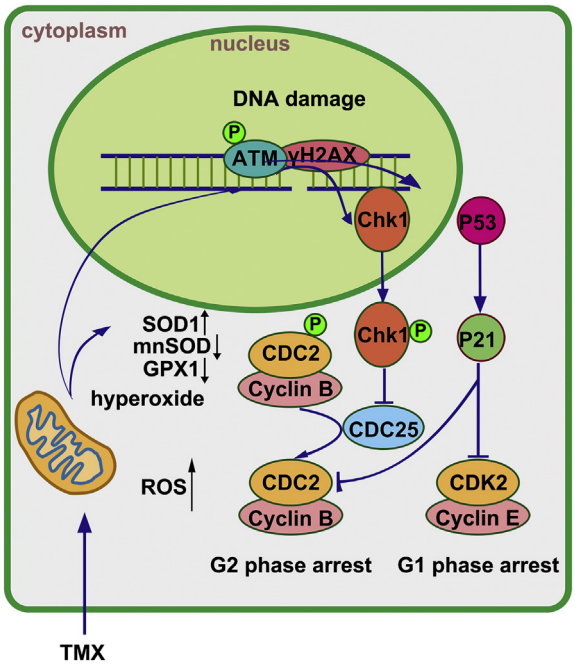

Fig. 8. Schematic representation of the ROS-dependent DNA damage checkpoint induced by TMX and subsequent G1 and G2 phase arrest in expanding blastocysts.

Conflict of interest

None

Acknowledgments

This research was supported by Basic Science Research Program through the National Research Foundation of Korea (NRF) funded by the government (MSIT) (No. 2018R1A2B6001173), Republic of Korea.

References

[1] A. Di Muccio, P. Fidente, D.A. Barbini, R. Dommarco, S. Seccia, P. Morrica, Application of solid-phase extraction and liquid chromatography-mass spectrometry to the determination of neonicotinoid pesticide residues in fruit and vegetables, J. Chromatogr. A 1108 (1) (2006) 1–6.
[2] P. Jeschke, R. Nauen, Neonicotinoids-from zero to hero in insecticide chemistry, Pest Manag. Sci. 64 (11) (2008) 1084–1098.
[3] N. Simon-Delso, V. Amaral-Rogers, L.P. Belzunces, J.M. Bonmatin, M. Chagnon, C. Downs, L. Furlan, D.W. Gibbons, C. Giorio, V. Girolami, D. Goulson, D.P. Kreutzweiser, C.H. Krupke, M. Liess, E. Long, M. McField, P. Mineau, E.A. Mitchell, C.A. Morrissey, D.A. Noome, L. Pisa, J. Settele, J.D. Stark, A. Tapparo, H. Van Dyck, J. Van Praagh, J.P. Van der Sluijs, P.R. Whitehorn, M. Wiemers, Systemic insecticides (neonicotinoids and fipronil): trends, uses, mode of action and metabolites, Environ. Sci. Pollut. Res. Int. 22 (1) (2015) 5–34.
[4] J. Babelova, Z. Sefcikova, S. Cikos, A. Spirkova, V. Kovarikova, J. Koppel, A.V. Makarevich, P. Chrenek, D. Fabian, Exposure to neonicotinoid insecticides induces embryotoxicity in mice and rabbits, Toxicology 392 (2017) 71–80.
[5] G.M. Telo, S.A. Senseman, E. Marchesan, E.R. Camargo, T. Jones, G. McCauley, Residues of thiamethoxam and chlorantraniliprole in rice grain, J. Agric. Food Chem. 63 (8) (2015) 2119–2126.
[6] D. Feil, M. Lane, C.T. Roberts, R.L. Kelley, L.J. Edwards, J.G. Thompson, K.L. Kind, Effect of culturing mouse embryos under different oxygen concentrations on subsequent fetal and placental development, J. Physiol. 572 (2006) 87–96 Pt 1.
[7] G. M. Harlow, P. Quinn, Foetal and placental growth in the mouse after pre-implantation development in vitro under oxygen concentrations of 5 and 20%, Aust. J. Biol. Sci. 32 (3) (1979) 363–369.
[8] L. Karagenc, Z. Sertkaya, N. Ciray, U. Ulug, M. Bahceci, Impact of oxygen concentration on embryonic development of mouse zygotes, Reprod. BioMed. Online 9 (4) (2004) 409–417.
[9] P.L. Wale, D.K. Gardner, Time-lapse analysis of mouse embryo development in oxygen gradients, Reprod. BioMed. Online 21 (3) (2010) 402–410.
[10] D.H. Betts, W.A. King, Genetic regulation of embryo death and senescence, Theriogenology 55 (1) (2001) 171–191.
[11] D.H. Betts, P. Madan, Permanent embryo arrest: molecular and cellular concepts, Mol. Hum. Reprod. 14 (8) (2008) 445–453.
[12] A. Jurisicova, B.M. Acton, Deadly decisions: the role of genes regulating programmed cell death in human preimplantation embryo development, Reproduction 128 (3) (2004) 281–291.
[13] M.R. Thomas, A.E. Sparks, G.L. Ryan, B.J. Van Voorhis, Clinical predictors of human blastocyst formation and pregnancy after extended embryo culture and transfer, Fertil. Steril. 94 (2) (2010) 543–548.
[14] D. De Zio, V. Cianfanelli, F. Cecconi, New insights into the link between DNA damage and apoptosis, Antioxid. Redox Signal. 19 (6) (2013) 559–571.
[15] S.H. Yan, J.H. Wang, L.S. Zhu, A.M. Chen, J. Wang, Thiamethoxam induces oxidative stress and antioxidant response in zebrafish (Danio Rerio) livers, Environ. Toxicol. 31 (12) (2016) 2006–2015.
[16] J. Guo, W.F. Lu, S. Liang, J.W. Choi, N.H. Kim, X.S. Cui, Peroxisome proliferator-activated receptor delta improves porcine blastocyst hatching via the regulation of fatty acid oxidation, Theriogenology 90 (2017) 266–275.
[17] J. Guo, M.H. Zhao, S. Liang, J.W. Choi, N.H. Kim, X.S. Cui, Liver receptor homolog 1 influences blastocyst hatching in pigs, J Reprod Dev 62 (3) (2016) 297–303.
[18] K.T. Lim, M.K. Gupta, S.H. Lee, Y.H. Jung, D.W. Han, H.T. Lee, Possible involvement of Wnt/beta-catenin signaling pathway in hatching and trophectoderm differentiation of pig blastocysts, Theriogenology 79(2) (2013) 284–90 e1–2.
[19] H. Wang, N.H. Kim, CDK2 is Required for the DNA damage Response during Porcine early Embryonic Development, Biol. Reprod. 95 (2) (2016) 31.
[20] D.K. Gardner, M. Lane, J. Stevens, T. Schlenker, W.B. Schoolcraft, Blastocyst score affects implantation and pregnancy outcome: towards a single blastocyst transfer, Fertil. Steril. 73 (6) (2000) 1155–1158.
[21] G.I. Perez, B.M. Acton, A. Jurisicova, G.A. Perkins, A. White, J. Brown, A.M. Trbovich, M.R. Kim, R. Fissore, J. Xu, A. Ahmady, S.G. D'Estaing, H. Li, W. Kagawa, H. Kurumizaka, S. Yokoyama, H. Okada, T.W. Mak, M.H. Ellisman, R.F. Casper, J.L. Tilly, Genetic variance modifies apoptosis susceptibility in mature oocytes via alterations in DNA repair capacity and mitochondrial ultrastructure, Cell Death Differ. 14 (3) (2007) 524–533.
[22] H.S. Yuh, D.H. Yu, M.J. Shin, H.J. Kim, K.B. Bae, D.S. Lee, H.C. Lee, W.K. Chang, S.B. Park, S.G. Lee, H.D. Park, J.H. Ha, B.H. Hyun, Z.Y. Ryoo, The effects of various antioxidants on the development of parthenogenetic porcine embryos, In Vitro Cell. Dev. Biol. Anim. 46 (2) (2010) 148–154.
[23] H. Wang, Y. Luo, Z. Lin, I.W. Lee, J. Kwon, X.S. Cui, N.H. Kim, Effect of ATM and HDAC Inhibition on Etoposide-Induced DNA damage in Porcine early Preimplantation Embryos, PLoS One 10 (11) (2015) e0142561.
[24] J. Bartek, J. Lukas, Pathways governing G1/S transition and their response to DNA damage, FEBS Lett. 490 (3) (2001) 117–122.
[25] T. Kishimoto, Entry into mitosis: a solution to the decades-long enigma of MPF, Chromosoma 124 (4) (2015) 417–428.
[26] X. Fan, J.J. Chen, Role of Cdk1 in DNA damage-induced G1 checkpoint abrogation by the human papillomavirus E7 oncogene, Cell Cycle 13 (20) (2014) 3249–3259.
[27] K.S. El-Gendy, N.M. Aly, F.H. Mahmoud, A. Kenawy, A.K. El-Sebae, The role of vitamin C as antioxidant in protection of oxidative stress induced by imidacloprid, Food Chem. Toxicol. 48 (1) (2010) 215–221.
[28] W. Ge, S. Yan, J. Wang, L. Zhu, A. Chen, J. Wang, Oxidative stress and DNA damage induced by imidacloprid in zebrafish (Danio rerio), J. Agric. Food Chem. 63 (6) (2015) 1856–1862.
[29] S. Yan, J. Wang, L. Zhu, A. Chen, J. Wang, Toxic effects of nitenpyram on antioxidant enzyme system and DNA in zebrafish (Danio rerio) livers, Ecotoxicol. Environ. Saf. 122 (2015) 54–60.
[30] X. Wang, A. Anadon, Q. Wu, F. Qiao, I. Ares, M.R. Martinez-Larranaga, Z. Yuan, M.A. Martinez, Mechanism of neonicotinoid toxicity: impact on oxidative stress and metabolism, Annu. Rev. Pharmacol. Toxicol. 58 (2018) 471–507.
[31] S. Mitra, I. Boldogh, T. Izumi, T.K. Hazra, Complexities of the DNA base excision repair pathway for repair of oxidative DNA damage, Environ. Mol. Mutagen. 38 (2–3) (2001) 180–190.
[32] N. Foray, D. Marot, A. Gabriel, V. Randrianarison, A.M. Carr, M. Perricaudet, A. Ashworth, P. Jeggo, A subset of ATM- and ATR-dependent phosphorylation events requires the BRCA1 protein, EMBO J. 22 (11) (2003) 2860–2871.
[33] N. Driessens, S. Versteyhe, C. Ghaddhab, A. Burniat, X. De Deken, J. Van Sande, J.E. Dumont, F. Miot, B. Corvilain, Hydrogen peroxide induces DNA single- and double-strand breaks in thyroid cells and is therefore a potential mutagen for this organ, Endocr. Relat. Cancer 16 (3) (2009) 845–856.
[34] J.R. Stone, S. Yang, Hydrogen peroxide: a signaling messenger, Antioxid. Redox Signal. 8 (3–4) (2006) 243–270.
[35] J. Reichenbach, R. Schubert, C. Schwan, K. Muller, H.J. Bohles, S. Zielen, Antioxidative capacity in patients with ataxia telangiectasia, Clin. Exp. Immunol. 117 (3) (1999) 535–539.
[36] M. Yi, M.P. Rosin, C.K. Anderson, Response of fibroblast cultures from ataxia-telangiectasia patients to oxidative stress, Cancer Lett. 54 (1–2) (1990) 43–50.
[37] A. Barzilai, G. Rotman, Y. Shiloh, ATM deficiency and oxidative stress: a new dimension of defective response to DNA damage, DNA Repair (Amst) 1 (1) (2002) 3–25.
[38] D.J. Watters, Oxidative stress in ataxia telangiectasia, Redox Rep. 8 (1) (2003) 23–29.
[39] A. Sancar, L.A. Lindsey-Boltz, K. Unsal-Kacmaz, S. Linn, Molecular mechanisms of mammalian DNA repair and the DNA damage checkpoints, Annu. Rev. Biochem. 73 (2004) 39–85.
[40] D. Delia, E. Fontanella, C. Ferrario, L. Chessa, S. Mizutani, DNA damage-induced cell-cycle phase regulation of p53 and p21waf1 in normal and ATM-defective cells, Oncogene 22 (49) (2003) 7866–7869.
[41] M. Thanasoula, J.M. Escandell, N. Suwaki, M. Tarsounas, ATM/ATR checkpoint activation downregulates CDC25C to prevent mitotic entry with uncapped telomeres, EMBO J. 31 (16) (2012) 3398–3410.
[42] G. He, Z.H. Siddik, Z. Huang, R. Wang, J. Koomen, R. Kobayashi, A.R. Khokhar, J. Kuang, Induction of p21 by p53 following DNA damage inhibits both Cdk4 and Cdk2 activities, Oncogene 24 (18) (2005) 2929–2943.
[43] E.M. Kim, J.K. Park, S.G. Hwang, W.J. Kim, Z.G. Liu, S.W. Kang, H.D. Um, Nuclear and cytoplasmic p53 suppress cell invasion by inhibiting respiratory complex-I activity via Bcl-2 family proteins, Oncotarget 5 (18) (2014) 8452–8465.
[44] D.R. Green, G. Kroemer, Cytoplasmic functions of the tumour suppressor p53, Nature 458 (7242) (2009) 1127–1130.
[45] N. Abella, S. Brun, M. Calvo, O. Tapia, J.D. Weber, M.T. Berciano, M. Lafarga, O. Bachs, N. Agell, Nucleolar disruption ensures nuclear accumulation of p21 upon DNA damage, Traffic 11 (6) (2010) 743–755.
[46] J. Cmielova, M. Lesna, M. Rezacova, Subcellular localization of proteins responding to mitoxantrone-induced dna damage in leukaemic cells, Folia Biol. (Praha) 61 (2) (2015) 60–65.
[47] S.K. Adiga, M. Toyoshima, K. Shiraishi, T. Shimura, J. Takeda, M. Taga, H. Nagai, P. Kumar, O. Niwa, p21 provides stage specific DNA damage control to preimplantation embryos, Oncogene 26 (42) (2007) 6141–6149.